A Three-Dimensional Structural Model for Predicting Magnetic Exchange and Hydrogen Positions in Bis-μ-Hydroxido Cu(II) Dimers

Stefani Gamboa-Ramirez, Khalil Youssef, Rafaello Papadakis, Michel Giorgi, Sylvain Bertaina, A. Jalila Simaan, Maylis Orio

A 3D Structural Model for Predicting Magnetic Exchange and Hydrogen Positions in Bis-μ-Hydroxido Cu(II) Dimers

Stefani Gamboa-Ramirez,[a] Khalil Youssef,[a] Rafaello Papadakis,[a]† Michel Giorgi,[b] Sylvain Bertaina,[c] A. Jalila Simaan,[a] and Maylis Orio*[a]

[a] Dr. S. Gamboa-Ramirez, Dr. K. Youssef, Dr. R. Papadakis, Dr. A. J. Simaan, Dr. M. Orio
Aix Marseille Univ, CNRS, Centrale Med, iSm2, Marseille, France
E-mail: maylis.orio@univ-amu.fr
† Current address: Swedish University of Agricultural Sciences, Uppsala, Sweden
[b] Dr. M. Giorgi
Aix Marseille Univ, CNRS, Centrale Med, FSCM, Marseille, France
[c] Dr. S. Bertaina
Aix Marseille Univ, CNRS, Université de Toulon, IM2NP, Marseille France
Supporting information for this article is given via a link at the end of the document.

Abstract: The magnetic properties of bis-μ-hydroxido copper(II) complexes were investigated with a focus on the correlation between structural parameters and exchange coupling constants (*J*). Beyond the classical Cu-O-Cu bridging angle (θ), we examined the hydroxido hydrogen out-of-plane angle (α) as a critical parameter. Using BS-DFT calculations and *J*-decomposition analysis on a benchmark complex, we showed that the kinetic exchange contribution governs the α-dependence of magnetic coupling. A three-dimensional magneto-structural correlation incorporating both θ and α was developed and validated against 22 structurally diverse dimers spanning ferromagnetic to antiferromagnetic regimes. Our model achieved a 15-fold improvement in predictive accuracy and correctly reproducing the sign of *J* in all cases. Notably, it enables estimation of the out-of-plane angle α, and thus the bridging hydrogen positions, often unresolved in X-ray diffraction data. Our findings highlight that bridging hydrogen position uncertainties are a major error source in computational magnetochemistry, offering a refined approach to predict magnetic behavior and enhance computational accuracy.

Introduction

Magnetic systems are crucial in many applications, including data storage, energy conservation or quantum computing.[1] Polynuclear transition metal complexes featuring magnetic interactions are a central topic in molecular magnetism. When the unpaired electrons of two or more open-shell centers are in close proximity, a magnetic interaction becomes operative.[2] This phenomenon is described by the exchange coupling constant, *J*, which reports the strength and nature of this interaction. *J* is usually described by the Heisenberg-Dirac Van Vleck Hamiltonian (HDvV)[3–6] as follows:

$$\hat{H}^{HDvV} = -2\sum_{i<j} J_{i,j}\hat{S}_i\hat{S}_j \quad (1)$$

where $J_{i,j}$ is the exchange coupling constant operative between center *i* and *j*, defined by their local spin operators $\hat{S}_i$ and $\hat{S}_j$, respectively. Understanding how the structure shapes the magnetic interaction in small systems is a prerequisite to predict the magnetic behavior of larger and more complicated frameworks. In this context, dinuclear copper(II) complexes provide the most straightforward case study of the magnetic interaction as it involves only one unpaired electron per metal center. The magnetic exchange between two $3d^9$ Cu^{II} ions (S_{Cu} = ½) leads either to *i*) a triplet ground spin state (S = 1) and a singlet excited spin state (S = 0) with an energy separation of 2*J, J* being positive or, *ii*) a singlet ground spin state and a triplet excited spin state with an energy separation of 2*J, J* being negative (Figure 1). The magnetic properties of dinuclear copper(II) complexes have been thoroughly studied over the years using experimental and computational approaches.[2,7–23] Many factors can tune the magnetic interaction of paramagnetic centers in close vicinity, and small modifications in distances and angles around the metal centers can trigger drastic changes in the sign and magnitude of *J*.

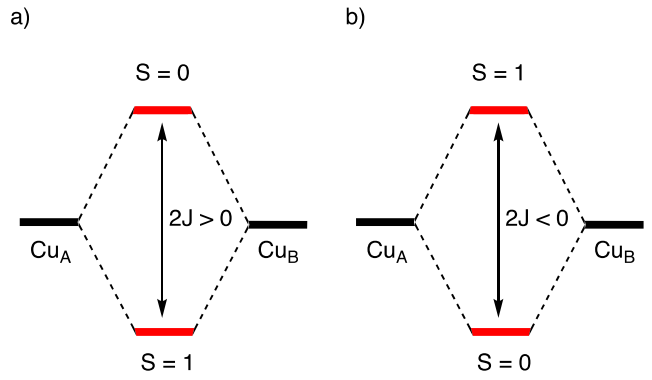

Figure 1. Schematic representation of the a) ferromagnetic and b) antiferromagnetic interaction in a dinuclear copper(II) complex. In this model, 2*J* is defined as: E(S=0)−E(S=1).

The pioneering work of Hatfield and Hodgson describing the magneto-structural correlation between a geometrical parameter, the Cu-O-Cu (θ), and the exchange coupling constant *J*, in a series of bis-μ-hydroxido copper(II) dimers opened-up a new avenue for molecular magnetism.[15] Computational studies based on density functional theory (DFT) methods from Ruiz and co-workers further supported the results experimentally observed by Hatfield and Hodgson.[11] They showed that θ was not the only geometrical parameter able to change the sign and magnitude of *J*. Their studies revealed the main role played by other structural parameters such the hinge distortion of the {Cu_2O_2} central framework and the out-of-plane angle (α) in hydroxido and alkoxo complexes (Figure 2).[8,9] Since then, other studies have reported the importance of α.[24,25] Given these earlier findings, it is logical to conclude that achieving a dependable theoretical description of μ-hydroxido dinuclear copper(II) complexes hinges on accurately accounting for the position of the hydroxido hydrogen. Additionally, the α angle for bis-μ-hydroxido metal complexes is strongly controlled by their ability to form hydrogen bonds with the surrounding counterions. Unfortunately, this aspect has not been considered in most experimental and computational studies, even though it has been proven to impact the results significantly.[13,26–33]

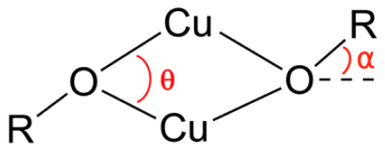

Figure 2. Schematic representation of the out-of-plane angle, α and the Cu-O-Cu angle, θ in a dinuclear copper(II) complex with R = H, OCH_3 or OPh moiety.

Quantum chemistry has become crucial for the precise description of electronic structures. However, accurately predicting the exchange coupling constant *J* using computational methods remains challenging.[34] Among all the state-of-the-art computational methods to predict *J*, Broken-Symmetry (BS) DFT in its Kohn-Sham (KS) formulation[35] appears as the method of choice to predict magnetic interactions.[29] However, the BS approach fails to capture the correct spin symmetry. This limitation can be addressed using spin projection schemes, with Yamaguchi's method[36] which incorporates spin expectation values from both high-spin and broken-symmetry solutions - proving effective when spin polarization effects are weak.[37,38]

$$J = \frac{E_{BS} - E_{HS}}{\langle \hat{S}^2 \rangle_{HS} - \langle \hat{S}^2 \rangle_{BS}} \quad (2)$$

where E_{BS} and E_{HS} stand for the broken-symmetry and high-spin energies, respectively, while $\langle S^2 \rangle_{HS}$ and $\langle S^2 \rangle_{BS}$ are the spin expectation values for the high-spin and broken-symmetry states, respectively.

A critical limitation in crystallographic studies of hydroxido-bridged complexes is the difficulty in accurately locating hydrogen positions from X-ray diffraction, particularly for the bridging OH groups that determine the out-of-plane angle, α. In this work, we address this challenge by demonstrating that magnetic properties can provide accurate information about these hydrogen positions. We report the theoretical investigation of a series of bis-μ-hydroxido copper(II) dimers $[Cu_2(OH)_2L_2]^{2+}$, featuring diverse counterions, ligand frameworks, and magnetic interactions. Using computational approaches such as BS-DFT and *J*-decomposition path, [39,40] we examine the significance of the out-of-plane angle (α) and establish a three-dimensional magneto-structural correlation linking α, θ, and *J*. This correlation offers a method to infer hydrogen positions that are often unresolved in crystallographic data.

Results and Discussion

Experimental characterization of a reference bis-μ-hydroxido copper(II) dimer

To establish a reliable benchmark for our study on the influence of the out-of-plane angle, α, we first selected complex **1**, $Cu_2(OH)_2(bipy)_2(ClO4)_2$ (bipy = 2,2'-bipyridine), as our reference complex (Figure 3, a). This choice was motivated by the availability of multiple structural reports in the literature, providing a robust foundation for comparison.[41-48] Complex **1** was synthesized following a protocol reported in the literature and recrystallized to confirm its chemical identity (see Suplementary Information for details). Additionally, we measured its magnetic susceptibility to

obtain a reliable experimental value of the exchange coupling constant, *J*, for comparison with our computational results. The temperature dependence of the magnetic susceptibility of complex **1** was measured in the 2-300 K temperature range under an applied field of 1 T. The presence of a ferromagnetic interaction was evidenced by the $\chi_m T$ *vs*. T plot (Figure 3, b) where χ_m represents the magnetic susceptibility per Cu_2 entity. The room temperature $\chi_m T$ value lies at 0.80 $cm^3.mol^{-1}.K$ above the threshold value of $\chi_m T$ = 0.749 $cm^3.mol^{-1}.K$ which is expected for two non-interactive Cu(II) ions.[2] By cooling down the sample, $\chi_m T$ values continuously increase due to depopulation of the excited state until reaching a maximum value of 1.03 $cm^3.mol^{-1}.K$ at 15K which corresponds to the temperature range where the singlet excited state is fully depopulated.

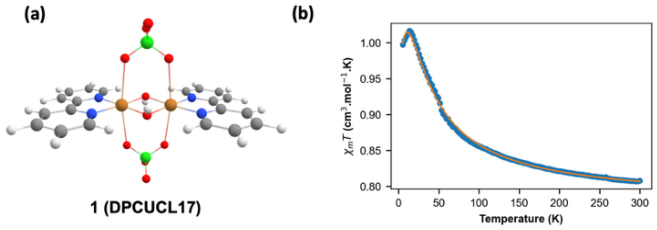

Figure 3. (a) Molecular structure and (b) $\chi_m T$ vs T plot of complex **1**, at 1 T. The solid orange line represents the best-simulated fit.

Magnetic data were analyzed using Equation (1)**,** with 2*J* being the singlet-triplet energy difference. To evaluate the magnetic constant, the experimental susceptibility curves were fitted using the Bleaney-Bowers equation for dinuclear models considering one unpaired electron per paramagnetic center (S = ½):[49]

$$\chi = \frac{2Ng^2\beta^2}{kT[3+\exp(-2J/kT)]} \quad (3)$$

The best fitting parameter was obtained by minimizing the agreement factor R:

$$R = \frac{\Sigma(\chi^{calc}{}_T - \chi^{exp}{}_T)^2}{\Sigma(\chi^{exp}{}_T)^2} \quad (4)$$

Using Equation (3), the fitting procedure provided *J* = +16 cm^{-1} with R = 9.00 x 10^{-6} for complex **1**.

Effect of the out-of-plane angle

To assess the performance of BS-DFT[35] for predicting *J* values of bis-μ-hydroxido copper(II) complexes, a calibration study using the single crystal X-ray diffraction data of complex **1** (CCDC 2539298) was performed using generalized gradient approximation (GGA), meta-GGA, hybrid GGA, meta-hybrid-GGA, double hybrid and range-separated hybrid functionals. Table 1 presents the computed J_{calc} values that were obtained using Equation (2) and the absolute deviation (AD) corresponding to the absolute difference between calculated and experimental exchange coupling constants such as:

$$AD = |J_{calc} - J_{exp}| \quad (5)$$

Our data show that pure DFT functional (GGA and meta-GGA) are far-off from the experimental value and predict the wrong nature of coupling. These results align with earlier research findings: functionals lacking any exact exchange disproportionately favor the broken-symmetry state over the high-spin state, resulting in exchange coupling constants that are overly negative when compared to experimental data. Conversely, hybrid functionals enhance the stability of high-spin states, with the degree of stabilization primarily determined by the proportion of Hartree-Fock exchange included and succeed in predicting the ferromagnetic coupling between the Cu(II) centers. Among them, TPSSh[55] predict correctly the sign of the exchange coupling constant and displays the lowest AD. It shows the best overall performance among all methods and appears to be the most suitable functional for describing the magnetic properties of our system, in agreement with previous findings on dinuclear transition metal complexes.[34,68] Scalar relativistic effects were evaluated using the zeroth-order regular approximation (ZORA)[56], and the results did not provide any major improvement in the prediction of *J* values compared to the non-relativistic case. Double hybrid (B2-PLYP)[65] and range-separated hybrid (LC-wPBE, ωB97X)[66,67] functionals were also assessed, providing results similar to those with the standard hybrid functional, consistent with earlier results.[10,69]

Table 1. BS-DFT exchange coupling constants (J_{calc}) and calculated absolute deviations (AD) for complex **1**.

Functional	%HF exchange	J_{calc} (cm^{-1})	AD (cm^{-1})
TPSS[50]	0	−31	35
BP86[51,52]	0	−39	47
PBE[53]	0	−41	49
BLYP[51,54]	0	−50	58
TPSSh[55]	10	37	21
TPSSh+ZORA[55,56]	10	47	31

B3LYP[54,57]	20	66	50
B3PW91[57,58]	20	67	51
TPSS0[59]	25	66	50
B1LYP[60]	25	70	54
PBE0[61-63]	25	71	55
BHandHLYP[64]	50	69	53
B2-PLYP[65]	53	63	47
LC-ωPBE[66]	0-100	80	64
ωB97X-D[67]	20-80	78	62
Expt.		**+16**	

To better understand the variation of J_{calc} as a function of the out-of-plane angle, α, we then performed a scan using the single crystal X-ray diffraction data of complex **1** varying only the α value from 0° to 90° with respect to the $\{Cu_2O_2\}$ plane. The theoretical results shown in Table S1 indicate that the sole variation of the α angle shifts both the strength and sign of J_{calc} from antiferromagnetic (−256 cm^{-1}) to ferromagnetic (+162 cm^{-1}) coupling when the hydroxido hydrogens go from the in-plane (α = 0°) to the out-of-plane (α = 90°) position. A threshold value of α = 38° represents the frontier between the two magnetic behaviors and is graphically illustrated in Figure 4. These results combined with complementary analyses (Figure S1-S7 and Tables S2-S6) agree with previous observations which identified that small out-of-plane angles favor antiferromagnetic coupling, whereas larger ones promote ferromagnetic interaction.[8,9]

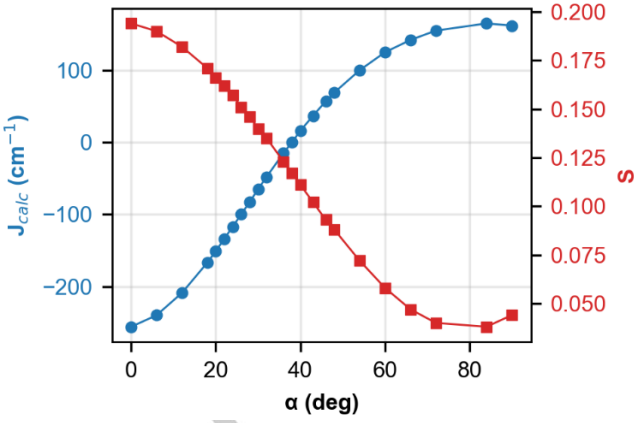

Figure 4. Variations of the BS-DFT computed exchange coupling constants (J_{calc}) and the orbital overlap (*S*) for complex **1** as a function of the out-of-plane angle (α).

The out-of-plane angle influences the exchange interaction by modulating the hybridization at the bridging oxygen atom, which dictates the overlap of the magnetic orbitals, *S*. Greater orbital localization, driven by this hybridization, thus reduces their overlap and weakens the exchange interaction. A maximum antiferromagnetic coupling is observed for an optimum orbital overlap, related to the minimum deviation of the hydroxido hydrogen from the $\{Cu_2O_2\}$ plane. At α = 0°, the overlap is the most efficient reaching its maximum value of *S* = 0.194 and leading to a strong antiferromagnetic coupling (J_{calc} = −256 cm^{-1}) while it decreases when the hydroxido hydrogen shifts from the in-plane position (Table S1). This phenomenon is graphically illustrated in Figure 5, where a higher delocalization of the magnetic orbitals is observed at α = 0° (in-plane situation). This delocalization gradually decreases until α reaches the out-of-plane position leading a minimum value of the orbital overlap, with *S* = 0.038 at α = 84°, which is directly correlated with the strongest ferromagnetic coupling (J_{calc} =+165 cm^{-1}).

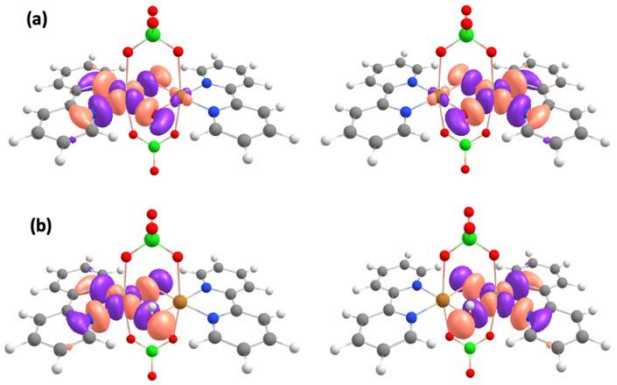

Figure 5. BS-DFT computed magnetic orbitals of complex **1** for the (a) in-plane situation (α = 0°) and (b) out-of-plane situation (α =84°).

Decomposition of the magnetic exchange coupling

The exchange coupling constant resulting from a magnetic interaction between two or more magnetic centers is not trivial, and different competing mechanisms define the sign and value of *J*. In this context, Ferré and co-workers introduced the decomposition of the exchange coupling constant *J* using a BS-DFT framework within the restricted open-shell formalism.[39,40,70] This approach intends to extract different physical contributions to the magnetic interaction for centrosymmetric systems. The *J* decomposition path allows to obtain three main physical contributions to the magnetic exchange coupling constant *i*) the ferromagnetic direct exchange (J_0), *ii*) the antiferromagnetic kinetic exchange (ΔJ_{ke}), and *iii*) the core polarization which can be either

positive or negative (ΔJ_{cp}). By adding up the contributions, pretty similar results to those resulting from the Yamaguchi approach are obtained[36], the difference between the two methods being denoted ΔJ_{other} such as:

$$J_T = J_0 + \Delta J_{ke} + \Delta J_{cp} + \Delta J_{other} \quad (6)$$

The first step of the *J*-decomposition path is to calculate the triplet and broken-symmetry states within the restricted open-shell formalism. From here, it is possible to extract the first contribution, J_0, which is always positive and describes the high spin configuration giving information on the ferromagnetic contribution to the J_T. Table 2 presents the computed direct exchange contributions (J_0) for a model complex of **1** varying α between 0 and 78˚. These results show that J_0 does not drastically change when α moves from the in-plane (α = 0˚, J_0 = +200 cm^{-1}) to the out-of-plane position (α = 78˚, J_0 = +152 cm^{-1}). Additionally, the J_0 values are far from those calculated with BS-DFT ($J_{BS\text{-}DFT}$), showing that J_0 alone cannot explain the important variation in the sign and magnitude of the computed *J* values as a function of the out-of-plane angle. To access the antiferromagnetic contribution, the kinetic exchange ΔJ_{ke}, the magnetic orbitals are relaxed in the unrestricted open-shell formalism. According to the results displayed in Table 2, ΔJ_{ke} drastically changes when α shifts from the in-plane to the out-of-plane position. Hence, the kinetic exchange is the main source responsible for the change in J_T as a function of the out-of-plane angle. Moreover, the sum of J_0 and ΔJ_{ke} gives a value very close to the $J_{BS\text{-}DFT}$, highlighting the importance of the kinetic exchange in regulating the sign and magnitude of the calculated *J* values when varying the α angle.[71] From this step, it is also possible to extract the Hubbard parameters: (*i*) U, corresponding to the repulsion of two electrons occupying the same site, and (*ii*) *t*, representing the hopping integral of one electron jumping from one site into the neighboring one. By convention, U and *t* always have different signs, with U being positive and *t* negative. When the absolute value of *t* increases, it promotes the population of the other magnetic center thus favoring the kinetic exchange, ΔJ_{ke}. In other words, when |*t*/U| increases, the ΔJ_{ke} contribution to J_T is more pronounced. Table 2 shows that when going from the in-plane (α = 0˚, *t* = −2252 cm^{-1}) to the out-of-plane (α = 78˚, *t* = −454 cm^{-1}) position, the absolute value of the hopping integral *t* decreases from while the term U increases, leading to a net decrease of both the absolute value of ΔJ_{ke} contribution and the antiferromagnetic character. Finally, the last physical contribution to the exchange coupling constant, the core polarization, ΔJ_{cp}, is obtained by relaxing the core orbitals and keeping the magnetic orbitals frozen in the high-spin and broken-symmetry states. As previously mentioned, the ΔJ_{cp} term can be either positive or negative, as reflected by the results shown in Table 2. All the ΔJ_{cp} values are positive for the system under investigation and slightly increase when α moves from the in-plane to the out-of-plane position. It is worth noting that the sum of the three contributions is very similar to the calculated value using the BS-DFT framework and the Yamaguchi approach, supporting the good performance of the decomposition path of the magnetic interaction in the present system (Figures S8-S9 and Tables S7-S10).

J, θ and α three-dimensional correlation

As mentioned earlier, both the strength and nature of the exchange interaction are influenced by two primary geometric parameters: the Cu-OH-Cu angle, θ and the out-of-plane angle, α. To achieve a more precise description of the magnetic properties of metal complexes featuring a bis-μ-hydroxido bridging ligands, it is essential to account for the position of the hydroxido hydrogens. Therefore, we established a magneto-structural correlation, described by Equation (7), that connects the θ and α angles with the calculated exchange coupling constants, J_{calc}, using complex **1** as the reference system and the computed data reported in Table S2:

$$J_{calc}(\theta, \alpha) = \sum_{i=0}^{2} \sum_{j=0}^{2} b_{ij} \theta^i \alpha^j \quad (7)$$

By defining the functional dependence of *J* on θ and α, our approach aims at enabling the reverse determination of α from experimental magnetic data.

Table 2. DFT calculated J_0, ΔJ_{ke}, ΔJ_{cp}, $J_{BS\text{-}DFT}$, *t* and U values for complex model of **1** as a function of α with a fixed θ value.

	α (˚), θ = 96.7˚								
	0	12	18	24	30	42	54	66	78
J_0 (cm^{-1})	200	188	177	166	156	142	138	144	152

ΔJ_{ke}(cm^{-1})	−469	−412	−360	−301	−240	−132	−61	−26	−15
$J_o + \Delta J_{ke}$ (cm^{-1})	−269	−224	−183	−135	−84	10	77	118	137
$J_o + \Delta J_{ke} + \Delta J_{cp}$ (cm^{-1})	−259	−212	−170	−119	−66	31	101	144	163
$J_{BS\text{-}DFT}$ (cm^{-1})	−256	−209	−167	−117	−65	30	100	142	160
t (cm^{-1})	−2552	−2379	−2214	−2013	−1787	−1415	−942	−600	−454
U (cm^{-1})	26839	26667	26510	26324	23117	30131	29022	27849	27516
$\lvert t/U \rvert$	0.095	0.089	0.084	0.076	0.077	0.047	0.032	0.022	0.016

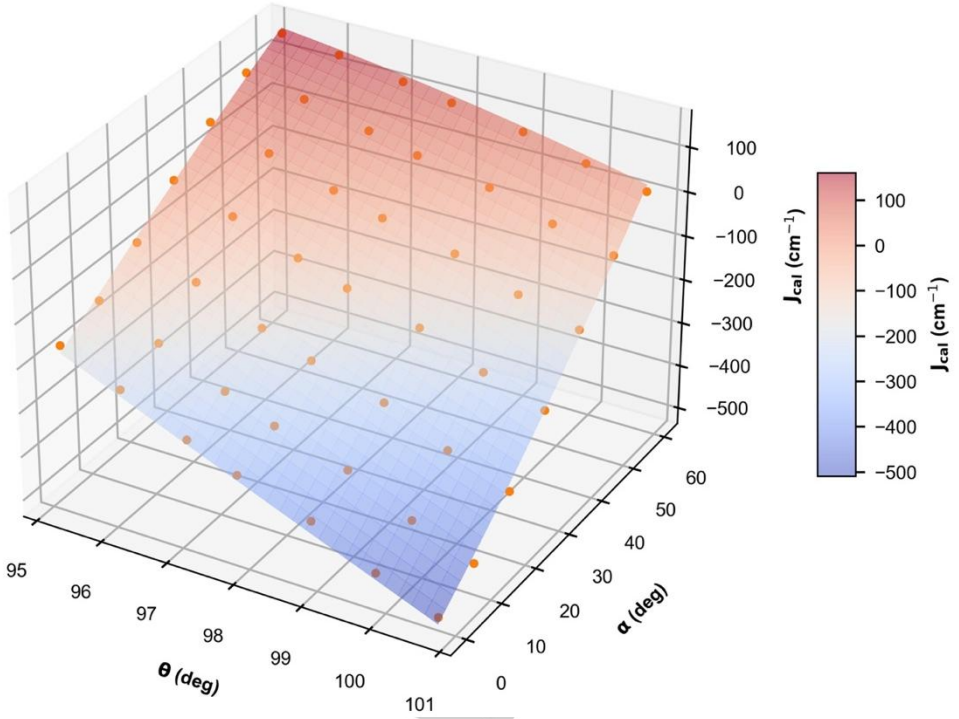

Figure 6. Three-dimensional correlation plot relating the Cu-OH-Cu (θ) and hydroxido out-of-plane angles (α) with the calculated exchange coupling constant (J_{calc}) using Equation (7) and complex **1** as the reference system.

Using Equation (7) and the b_{ij} coefficients listed in Table S11 provides the three-dimensional (3D) correlation graphically depicted in Figure 6. To assess the performance of the 3D correlation, we collected 22 bis-μ-hydroxido dinuclear copper(II) complexes that fulfilled the criteria of having well-defined crystal structures and exchange coupling constants (J_{exp}). Equation (7) establishes a direct relationship between the experimentally accessible quantities (Cu-OH-Cu angle and *J*) and the out-of-plane angle α, which encodes the position of hydrogen atoms at the bridging sites. This relationship enables us to invert the traditional approach: rather than using crystal structures to predict *J*, we use experimental *J* values to determine α from magnetic measurements, thereby determining hydrogen positions that cannot be reliably obtained from X-ray diffraction alone.

Figure 7 presents the set of complexes **2-9** which all display the same $[Cu_2(OH)_2(bipy)_2]^{2+}$ core (bipy = 2,2'-bipyridine) but feature various counterions: $CF_3SO_3^-$ (**2**), NO_3^- (**3**), HPO_4^- (**4**), NCS^- (**5**), $Au(CN)_4^-$ (**6**), BF_4^- (**7**), C4O4$^-$ (**8**), and SO_4^{2-} (**9**). Figure 8 shows the set of complexes **10-23** corresponding to bis-μ-hydroxido copper(II) dimers having different ligand frameworks and counter-ions. While complexes **2-9** display ferromagnetic couplings, complexes **10-23** present more diverse magnetic interactions, both in nature

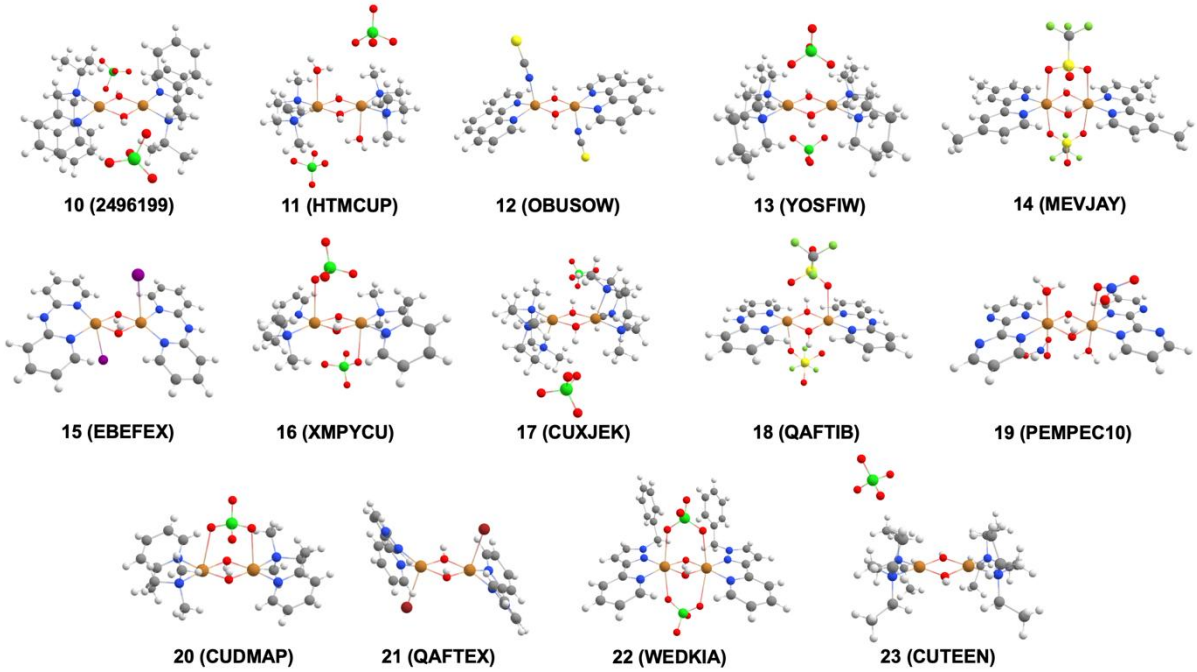

and strength, a prerequisite to assess the performance of our 3D correlation. Most complexes were retrieved from previously published studies with exception of the newly synthetized complex **10** that was examined experimentally in this work (see Suplementary Information for details). 5 of the listed complexes (**4**, **9**, **14**, **21** and **22**) display asymmetric Cu-OH-Cu angles (θ); therefore, the average θ value was used, following recommendations from previous computational studies (see Table S12).[25]

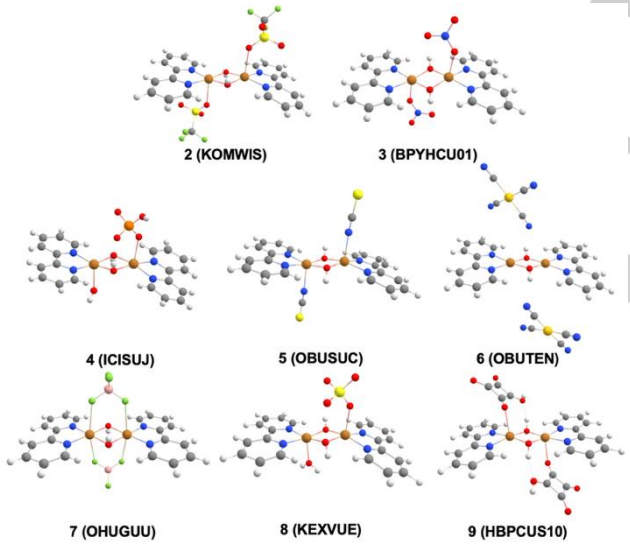

Figure 7. Molecular structures of the bis-μ-hydroxido copper(II) complexes with a $[Cu_2(OH)_2(bipy)_2]^{2+}$ core and different counter-ions.

The experimental values of both the Cu-OH-Cu angle (θ_{exp}) and the exchange coupling constant (J_{exp}) were used in combination with Equation (7) to estimate the optimum value of out-of-plane (α_{3D}) angle. After extracting the corresponding α_{3D} values from the 3D correlation, the out-of-plane angles were adjusted accordingly within the original crystal structure of each complex. Then, the computed exchange coupling constants using the fitted 3D α values, J_{3D}, were obtained BS-DFT computations. Finally, we computed the exchange coupling constants using the X-ray-determined values of α, $J_{X\text{-}ray}$ and we compared them to the values obtained using the optimum α_{3D} angle, J_{3D}, to evaluate the performance of the 3D correlation. The capability of 3D correlation to accurately predict exchange coupling constants was determined by evaluating the absolute difference (AD, Figure 9) using Equation (5). We also evaluated the absolute percentage deviations (APD) of the above parameters with respect to experimental results as follows (Figure S10):

$$APD = \left|\frac{J_{calc}-J_{exp}}{J_{exp}}\right| \times 100 \quad (8)$$

Mean absolute difference (MAD) and mean absolute percentage deviation (MAPD) using equations (**5**) and (**7**) were calculated such as:

$$MAD = \frac{1}{N}\sum_{i=1}^{N}\left|J_{calc} - J_{exp}\right| \quad (9)$$

$$MAPD = \frac{1}{N}\sum_{1=1}^{N}\left|\frac{J_{calc}-J_{exp}}{J_{exp}}\right| \times 100 \quad (10)$$

Table 3 and Figure 9 report the experimental exchange coupling constants (J_{exp}) and the computed values using either the original single crystal X-ray diffraction data ($J_{X\text{-}ray}$) or those with 3D-adjusted α angles (J_{3D}), along with their respective absolute differences ($AD_{X\text{-}ray}$ and AD_{3D}) and absolute percentage deviations ($APD_{X\text{-}ray}$ and AD_{3D}). To complement the evaluation of the 3D correlation, the mean absolute differences (MAD) and mean absolute percentage deviations (MAPD) were also assessed.

The quantitative analysis of Table 3 reveals the systematic improvement achieved by the 3D correlation across the entire dataset. The determination of the AD shows that using the optimum values of out-of-plane angle, α_{3D}, significantly improves the calculated exchange coupling constants,

Figure 8. Molecular structures of the bis-μ-hydroxido copper(II) complexes with different ligand frameworks and counter-ions.

predicting the correct nature of the magnetic interaction and moving towards a quantitative prediction of *J*. Focusing first on the $[Cu_2(OH)_2(bipy)_2]^{2+}$ series (complexes **2-9**), which represents a chemically homogeneous subset where only the counterion varies, an average AD_{3D} of 7 cm^{-1} is obtained compared to an average $AD_{X\text{-}ray}$ of 127 cm^{-1}. Within this series, complexes **5** (AD_{3D} = 1 cm^{-1}), **6** (AD_{3D} = 1 cm^{-1}), and **7** (AD_{3D} = 0 cm^{-1}) demonstrate near-perfect agreement between calculated and experimental values. These results are particularly noteworthy as they span a broad range of counterions, demonstrating that the 3D correlation successfully captures the subtle electronic modulations induced by different anions through their influence on the out-of-plane angle. The largest deviation within this series is observed for complex **4** (AD_{3D} = 18 cm^{-1}), which nonetheless represents a dramatic improvement over the $AD_{X\text{-}ray}$ value of 666 cm^{-1}, reducing the error by a factor of 37.

Beyond the bipy series, complexes **10-23** provide a stringent test of the 3D correlation's transferability, as they feature diverse ligand frameworks, coordination geometries, and magnetic behaviors ranging from antiferromagnetic (J_{exp} = −205 cm^{-1} for **23**) to ferromagnetic (J_{exp} = +117 cm^{-1} for **13**) couplings. Remarkably, the correlation performs consistently well across this heterogeneous set. Two complexes achieve perfect agreement: **16** and **21** (AD_{3D} = 0 cm^{-1}), both displaying antiferromagnetic couplings. Complex **14** also demonstrates excellent performance with AD_{3D} = 4 cm^{-1} for a ferromagnetic system. These results establish that the 3D correlation is not biased toward a particular coupling regime. The largest deviations are observed for complexes **13** (AD_{3D} = 33 cm^{-1}) and **23** (AD_{3D} = 28 cm^{-1}). In the case of **13**, the experimental value of J_{exp} = +117 cm^{-1} represents a ferromagnetic coupling, which lies at the extreme of the calibration range. For **23**, the antiferromagnetic character (J_{exp} = −205 cm^{-1}) places this complex near the boundary of the parameter space explored during calibration. Despite these larger absolute deviations, both complexes still benefit substantially from the 3D correction, with $AD_{X\text{-}ray}$ values of 396 and 737 cm^{-1} reduced to 33 and 28 cm^{-1}, respectively, representing improvements of 12- and 26-fold.

Table 3. Experimental Cu-OH-Cu (θ_{exp}) and 3D-extrapolated out of the plane (α_{3D}) angles, experimental (J_{exp}) and calculated ($J_{X\text{-}ray}$ and J_{3D}) exchange coupling constants with their respective absolute differences ($AD_{X\text{-}ray}$ and AD_{3D}), absolute percentage deviations ($APD_{X\text{-}ray}$ and APD_{3D}), mean absolute differences (MAD) and mean absolute percentage deviations (MAPD) for the selected bis-μ-hydroxido copper(II) complexes.

Complex	CCDC code	θ_{exp} (°)	J_{exp} (cm^{-1})	$J_{X\text{-}ray}$ (cm^{-1})	α_{3D} (°)	J_{3D} (cm^{-1})	$AD_{X\text{-}ray}$	AD_{3D}	$APD_{X\text{-}ray}$	APD_{3D}	Reference
2	KOMWIS	98.0	5	−10	47.4	11	15	6	300	120	[72]
3	BPYHCU01	95.4	74	132	43.6	65	58	9	78	12	[23]
4	ICISUJ	96.0	92	758	49.9	110	666	18	724	20	[32]
5	OBUSUC	97.2	15	44	47.5	14	29	1	193	7	[73]
6	OBUTEN	98.4	8	22	49.6	7	14	1	175	13	[73]
7	OHUGUU	97.4	22	95	46.7	22	73	0	332	0	[22]
8	KEXVUE	96.4	73	134	48.9	79	61	6	84	8	[72]
9	HBPCUS10	96.6	25	127	42.7	41	102	16	408	64	[20,74]
10	2496199	102.4	−152	−572	49.6	−144	420	8	276	5	This work
11	HTMCUP	101.6	−172	−420	44.0	−185	247	13	144	8	[21,22]
12	OBUSOW	97.0	12	50	43.4	3	38	9	317	75	[73]
13	YOSFIW	96.9	117	−279	57.6	84	396	33	338	28	[75]
14	MEVJAY	95.1	74	53	41.6	70	21	4	28	5	[76]
15	EBEFEX	98.5	−8	121	48.0	−10	129	12	1613	25	[77]
16	XMPYCU	100.5	−101	−139	46.5	−101	38	0	38	0	[78]
17	CUXJEK	100.1	−45	−131	50.6	−55	86	10	191	22	[79]
18	QAFTIB	99.3	42	139	56.7	58	97	16	231	38	[80]
19	PEMPEC10	95.6	57	125	42.2	75	68	18	119	32	[81]
20	CUDMAP	98.4	−5	16	48.0	−19	21	14	433	296	[82,83]

21	QAFTEX	99	−24	−22	48.3	−24	2	0	8	0	[80,84]
22	WEDKIA	95.2	41	83	37.8	34	42	7	102	17	[85]
23	CUTEEN	103.9	−205	−942	50.9	−177	737	28	360	14	[86]
MAD (cm^{-1})							**153**	**10**	-	-	
MAPD (%)							-	-	**295**	**37**	

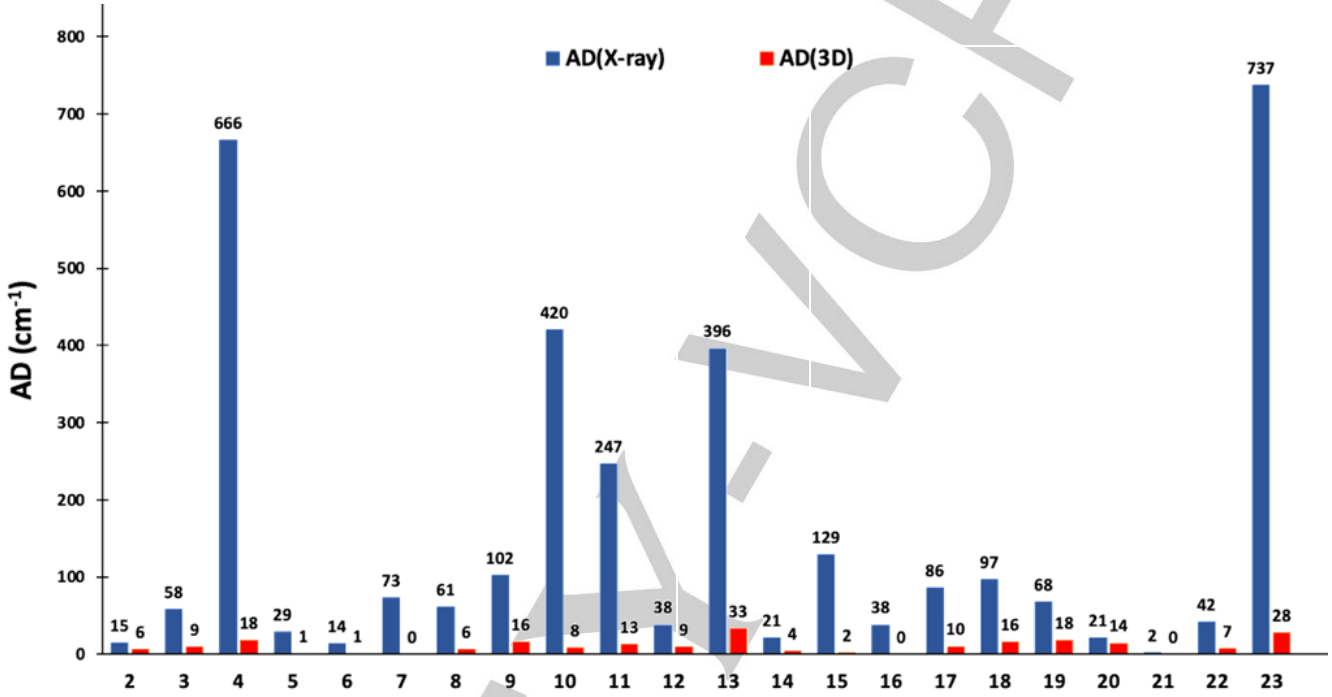

Figure 9. Comparison of the absolute differences between experimental and calculated *J* values using the out-of-planes angles from the single crystal X-ray diffraction data (AD(X-ray), blue bars) and the optimum values from 3D correlation (AD(3D), red bars).

Critically, the 3D correlation correctly predicts the sign of the magnetic interaction in all 22 cases examined. This systematic sign fidelity underscores the physical soundness of incorporating the out-of-plane angle into magneto-structural correlations. The overall statistics (MAD_{3D} = 10 cm^{-1} versus $MAD_{X\text{-}ray}$ = 153 cm^{-1}, and $MAPD_{3D}$ = 37% versus $MAPD_{X\text{-}ray}$ = 295%) demonstrate that the 3D correlation provides a robust and generalizable framework for predicting exchange coupling constants in bis-μ-hydroxido copper(II) dimers, regardless of the ancillary ligand environment or the nature and magnitude of the magnetic exchange.[87] The main achievement of this work is thus the establishment of a quantitative method to approximate hydrogen positions at bridging oxygen atoms from readily accessible experimental data. Our magneto-structural correlation represents a significant improvement over typical uncertainties in hydrogen positions from conventional refinement. Moreover, our approach requires only standard magnetometry measurements and crystallographic data for the heavy atoms, making it broadly applicable to the extensive family of hydroxido-bridged copper(II) complexes.

Conclusion

This work proposes a robust three-dimensional magneto-structural correlation for predicting exchange coupling constants in bis-μ-hydroxido copper(II) dimers by incorporating both the Cu-OH-Cu angle (θ) and the hydroxido out-of-plane angle (α). Through systematic BS-DFT calculations and *J*-decomposition analysis using complex **1** as a benchmark system, we demonstrated that the kinetic exchange contribution (ΔJ_{ke}) is the dominant factor governing the α-dependence of magnetic coupling. The main achievement of our study lies in the substantial improvement in predictive accuracy afforded by the 3D correlation. Validation against 22 structurally diverse bis-μ-hydroxido copper(II) complexes yielded a mean absolute deviation of only 10 cm^{-1}, compared to 153 cm^{-1} when using crystallographically determined α values. This 15-fold reduction in prediction error,

achieved without any system-specific reparameterization, demonstrates that the correlation captures the physics underlying magneto-structural relationships in this class of compounds. Importantly, our method correctly predicts the sign of the exchange interaction in all cases examined, spanning from antiferromagnetic to ferromagnetic couplings. This work also highlights a critical yet often overlooked source of computational error: the position of bridging hydrogen atoms. Single-crystal X-ray diffraction data typically provide unreliable H-atom coordinates, while standard DFT geometry optimizations may not accurately reproduce the subtle balance of forces - including hydrogen bonding with counterions - that determine α in the solid state. The 3D correlation offers a practical solution by extracting the optimal α value directly from the experimental θ and *J*, thereby circumventing the limitations inherent to both experimental and computational structure determination. Beyond its immediate application to structure determination, this work establishes a general methodology for using magnetic properties as structural probes, potentially extensible to other bridged systems where light atom positions are crystallographically ambiguous. More broadly, this study underscores the importance of treating bridging ligand geometry as an independent variable in magneto-structural correlations, rather than as a fixed structural constraint. The observation that counterion identity modulates the out-of-plane angle through hydrogen bonding interactions suggests that supramolecular engineering strategies could be employed to fine-tune magnetic properties without modifying the primary coordination sphere. The 3D correlation presented here provides the quantitative framework needed to guide such efforts and to accelerate the computational screening of candidate magnetic materials.

Experimental Section

General Experimental Procedure

All chemicals used in synthesizing the ligand and complexes were commercially available, as well as the solvents. All aqueous solutions were prepared using Milli-Q Ultrapure water. Elemental analyses were performed using the Thermo Finnigan EA 112 instrument. The results are provided with an absolute accuracy of 0.3% and validated for at least two analyses. ^{1}H and ^{13}C NMR spectra were recorded at 25° in a CDCl3 solution on a BRUKER Avance III nanobay spectrometer at 300 MHz. The letters following the chemical displacement δ, such as s, d, t, q, qt, and m, corresponding to singlet, doublet, triplet, quartet, quintet, and multiplet.

Synthesis of Copper Complexes

Complex 1 was obtained by adding dropwise a solution of $Cu(ClO_4)_2{\cdot}6H_2O$ (500 mg, 1.35 mmol, 1 eq) in water (30 mL with pH adjusted 9 by dropwise addition of 1 M NaOH) to a solution of 2,2'-bipyridine (210.7 mg, 1.35 mmol, 1 eq.) in MeOH (3 mL). A lavender precipitate was formed after 1 hour-stirring of the mixture. The powder was collected via vacuum filtration and washed with diethyl ether. 170 mg of crystals were recuperated after recrystallization from ACN/H_2O (5:1). Elemental analysis: Calculated for C20H18Cl2Cu2N4O10: C 35.73; H 2.70; N 8.33; Found: C 35.34; H 2.61; N 8.23.

Ligand of complex 10 (L10) was obtained by adding dropwise under Ar atmosphere a solution of isopropylbenzylamine (1.56 mL, 9.34 mmol, 1 eq.) to a solution of 2-pyridine-carboxy-aldehyde (1.00 g, 9.34 mmol, 1 eq.) in dry MeOH (5 mL). The reaction mixture was left to stir for 24 h. In the same pot, $NaBH_4$ (0.53 g, 14 mmol, 1.5 eq.) was added 2 times, and the reaction was left to stir for another 24 h. Finally, MeOH was evaporated under reduced pressure, and 25 mL of DCM and 25 mL of basic brine (pH = 11) were added. The organic phase was dried over $MgSO_4$, and the solvent evaporated under reduced pressure. The crude was purified by flash column chromatography with neutral alumina with cyclohexane/EtOAc (9:1) to yield 965.3 mg (43%) of yellowish oil. ^{1}H NMR (400 MHz, $CDCl_3$) δ 8.46 (dt, J = 5.0, 1.4 Hz, 1H), 7.66 – 7.57 (m, 2H), 7.42 – 7.34 (m, 2H), 7.33 – 7.27 (m, 3H), 7.22 – 7.17 (m, 1H), 7.12 – 7.07 (m, 1H), 3.79 (s, 0H), 3.75 (s, 2H), 3.62 (s, 2H), 2.99 – 2.82 (m, 1H), 1.10 (dd, J = 6.4, 5.3 Hz, 8H). ^{13}C NMR (101 MHz, $CDCl_3$) δ 161.68, 148.58, 140.63, 136.33, 128.61 – 127.98, 126.64, 121.96, 76.69, 54.69, 49.29, 22.89, 17.78.

Complex 10 was obtained by adding dropwise a solution of $Cu(ClO_4)_2{\cdot}6H_2O$ (451 mg, 1.2 mmol, 1 eq.) in absolute EtOH (4 mL) to a solution of **L10** (288.4 mg, 1.2 mmol, 1 eq.) in absolute EtOH (4 mL). A deep blue-violet precipitate was formed immediately after. The powder was collected via vacuum filtration and washed with diethyl ether. 350 mg of crystals were recuperated after recrystallization from ACN/H_2O (5:0.2). Elemental analysis: Calculated for

$C_{32}H_{42}Cl_2Cu_2N_4O_{10}$: C 45.72; H 5.04; N 6.77; Found: C 45.61; H 5.02; N 6.77.

Crystallographic structure determination

Crystals of complexes **1** and **10**, suitable for single crystal X-ray diffraction analysis were measured on a Bruker Apex2 diffractometer at 100K at the MoKα radiation (λ=0.71073 Å) for **1** and on a Rigaku Oxford Diffraction SuperNova diffractometer at room temperature at the CuKα radiation (λ=1.54184 Å) for **10**. Data collection reduction and multiscan correction were performed with APEX2 (Bruker) for **1** and with CrysAlisPro (Rigaku Oxford Diffraction) for **10**. Using Olex2,[88] the structures were solved by intrinsic phasing methods with SHELXT.[89] Using Olex2, all atoms in **1**, including hydrogens, were refined with NoSpherA2[90] while all non-H atoms in **10** were refined with SHELXL.[91] All H-atoms in **10** found experimentally (except those of the acetonitrile moiety) but reintroduced at geometrical positions and refined as riding atoms with their Uiso parameters constrained to 1.2Ueq(parent atom) for the CH groups and to 1.5Ueq(parent atom) for the CH_3 and the OH groups. Relevant crystallographic data are presented in Table S13. Crystal structures have been deposited at the Cambridge Crystallographic Data Centre. Deposition Numbers 2539298 and 2496199 for **1** and **10**, respectively, contain the supplementary crystallographic data for this paper (https://www.ccdc.cam.ac.uk/services/structures?id=doi:10.1002/ejic.202500589) These data are provided free of charge by the joint Cambridge Crystallographic Data Centre and Fachinformationszentrum Karlsruhe (http://www.ccdc.cam.ac.uk/structures) Access Structures service.

Magnetic Studies

The magnetic properties were performed with a SQUID magnetometer MPMS-XL from Quantum Design in the temperature range from 2 to 380K. The magnetic contribution of the sample holder bag was removed beforehand. A primary vacuum in the bag was performed to remove the magnetic contribution of the sold oxygen. The detection was made by transporting the sample through the gradiometer using the Reciprocating Sample Option (RSO) at a frequency of 1Hz.

Computational Details

All calculations were performed using the ORCA program package 4.0.[92] We performed a benchmark study using the single crystal X-ray diffraction data of complex **1** and single-point BS-DFT calculations[35] with the def2-TZVP[93,94] basis set to compute exchange coupling constants, J_{calc}, with a large variety of functionals. Spin configurations for the BS-DFT calculations were generated with the "FlipSpin" feature of ORCA. Resolution of the identity (RI) approximation in the Split-RI-J variant[95] with the appropriate Coulomb fitting sets[96], increased integration grids (Grid4 in ORCA convention) and VeryTight SCF convergence criteria were used. Scalar relativistic effects were also assessed using the zeroth-order regular approximation (ZORA)[56] in combination with the ZORA-def2-TZVP basis set.[97] All calculations following the benchmark study were single-point BS-DFT calculations using the hybrid functional TPSSh[55] and the def2-TZVP basis set.[93,94] The effect of the hydroxido out-of-plane angle on the J_{calc} values was assessed by scanning values ranging from 0 to 90˚ in the crystal structure of complex **1**. The *J*-decomposition path implemented in the ORCA program [39,40,70] was performed to correlate the out-of-plane angle with the sign and value of the J_{calc} values. Starting from the single crystal X-ray diffraction data, several models of complex **1** were constructed using a fixed θ = 96.7˚ and varying α angles between 0˚ and 78˚. To construct the 3D magneto-structural correlation, additional models of complex **1** were considered scanning two different angles: (*i*) the Cu-OH-Cu bridging angle from 95 to 101˚ and (*ii*) the hydroxido out-of-plane angle from 0 to 60˚. The performance of the 3D correlation was assessed using the single crystal X-ray diffraction data of the 22 selected complexes. Only the hydroxido out-of-plane angles were adjusted to the optimum values determined using Equation(7). Natural Bond Orbital (NBO) analysis[98] was performed using the BP86[51,52] functional with the def2-TZVP[93,94] basis sets using the Gaussian 09 program package.[99] Spin density plots and molecular orbitals were generated using the orca_plot utility and visualized with the Chemcraft program.[100]

Supporting Information

The authors have cited additional references within the Supporting Information.[101-104] The Supporting Information includes additional computational and experimental data as well as cartesian coordinates.

Acknowledgements

The authors gratefully acknowledge financial support of this work by the French National Research Agency and the Deutsche Forschungsgemeinschaft (CUBISM, grant no. ANR-18 CE092_0040_01/DFG project no. 406697875), and from the France-Germany Hubert Curien Program German Academic Exchange Service (DAAD) (Procope 2019–2020 project 42525PB/ DAAD project 57445526). This work was also supported by the French National Research Agency (COSACH, grant no. ANR-22-CE07-0032) and the CNRS research infrastructure INFRANALYTICS (FR2054). The authors gratefully acknowledge Dr. Sébastien Pillet for his valuable contribution to the preliminary crystal structure refinement.

Keywords: copper complexes • magnetic interaction • density functional theory • magneto-structural correlation

[1] (a) B. Zhang, P. Lu, R. Tabrizian, P. X. Feng, Y. Wu, "2D Magnetic heterostructures: spintronics and quantum future", *NPJ Spintronics* **2024**, *2*, 1, (b) E. Elahi, M. A. Khan, M. Suleman, A. Dahshan, S. Rehman, H. W. Khalil, M. A. Rehman, A. M. Hassan, G. Koyyada, J. H. Kim, M. F. Khan, "Recent innovations in 2D magnetic materials and their potential applications in the modern era", *Mater. Today* **2023**, *72*, 183–206.

[2] O. Kahn, Molecular Magnetism, VCH: New York, NY **1993**.

[3] W. Heisenberg, "Mehrkörperproblem und Resonanz in der Quantenmechanik." *Z. Phys.* **1926**, *38*, 411–426.

[4] W. Heisenberg, "Zur Theorie des Ferromagnetismus". *Z. Phys.* **1928**, *49*, 619–636.

[5] P. A. M. Dirac, "Quantum Mechanics of Many-Electron Systems", *Proc. R. Soc. Lond. Ser. Contain. Pap. Math. Phys. Character* **1929**, *123*, 714–733.

[6] J. H. van Vleck, "The Theory of Electric and Magnetic Susceptibilities", *Nature* **1932**, *130*, 490–491.

[7] E. Coronado, "Molecular Magnetism: From Chemical Design to Spin Control in Molecules, Materials and Devices", *Nat. Rev. Mater.* **2020**, *5*, 87–104.

[8] E. Ruiz, P. Alemany, S. Alvarez, J. Cano, "Toward the Prediction of Magnetic Coupling in Molecular Systems: Hydroxo- and Alkoxo-Bridged Cu(II) Binuclear Complexes", *J. Am. Chem. Soc.* **1997**, *119*, 1297–1303.

[9] E. Ruiz, P. Alemany, S. Alvarez, J. Cano, "Structural Modeling and Magneto−Structural Correlations for Hydroxo-Bridged Copper(II) Binuclear Complexes", *Inorg. Chem.* **1997**, *36*, 3683–3688.

[10] E. Ruiz, "Exchange Coupling Constants Using Density Functional Theory: Long-Range Corrected Functionals", *J. Comput. Chem.* **2011**, *32*, 1998–2004.

[11] E. Ruiz, "Theoretical Study of the Exchange Coupling in Large Polynuclear Transition Metal Complexes Using DFT Methods", in *Principles and Applications of Density Functional Theory in Inorganic Chemistry II*, N. Kaltsoyannis, J. E. McGrady (Eds.), Structure and Bonding, Springer: Berlin, Heidelberg, **2004**, 71–102.

[12] J. P. Malrieu, R. Caballol, C. J. Calzado, C. de Graaf, N. Guihéry, "Magnetic Interactions in Molecules and Highly Correlated Materials: Physical Content, Analytical Derivation, and Rigorous Extraction of Magnetic Hamiltonians", *Chem. Rev.* **2014**, *114*, 429–492.

[13] M. Julve, A. Gleizes, L. M. Chamoreau, E. Ruiz, M. Verdaguer, "Antiferromagnetic Interactions in Copper(II) μ-Oxalato Dinuclear Complexes: The Role of the Counterion", *Eur. J. Inorg. Chem.* **2018**, *2018*, 509–516.

[14] J. A. Barnes, D. J. Hodgson, W. E. Hatfield, "Magnetic Properties of a Series of Hydroxo-Bridged Complexes of 2,2'-Dipyridyl and Copper(II)", *Inorg. Chem.* **1972**, *11*, 144–148.

[15] V. H. Crawford, H. Wayne Richardson, J. R. Wasson, D. J. Hodgson, W. E. Hatfield, "Relation between the Singlet-Triplet Splitting and the Copper-Oxygen-Copper Bridge Angle in Hydroxo-Bridged Copper Dimers", *Inorg. Chem.* **1976**, *15*, 2107–2110.

[16] Y.-Q. Zheng, J.-L. Lin, "Hydroxo-Bridged Tetranuclear CuII Complexes: {[Cu(Bpy)(OH)]$_4$Cl$_2$}Cl$_2$·6H2O and {[Cu(Phen)(OH)]$_4$(H$_2$O)$_2$}]Cl$_4$·4H$_2$O", *Z. Anorg. Allg. Chem.* **2002**, *628*, 203–208.

[17] S. Sain, T. K. Maji, G. Mostafa, T.-H. Lu, J. Ribas, X. Tercero, N. Ray Chaudhuri, "Magneto Structural Correlations of a 'Stepped-Wise' Discrete Tetranuclear Unit of Copper(II), [Cu$_4$(μ$_2$-OH)$_2$((μ$_3$-OH)$_2$(2,2′-Bipy)$_4$Cl$_2$]Cl$_2$·6H$_2$O", *Polyhedron* **2003**, *22*, 625–631.

[18] J. P. Collman, M. Zhong, C. Zhang, S. Costanzo, "Catalytic Activities of Cu(II) Complexes with Nitrogen-Chelating Bidentate Ligands in the Coupling of Imidazoles with Arylboronic Acids", *J. Org. Chem.* **2001**, *66*, 7892–7897

[19] C. Harris, E. Sinn, W. Walker, P. Woolliams, "Nitrogenous Chelate Complexes of Transition Metals. V. Binuclear Hydroxybridged Copper(II) Complexes of 1,10-Phenanthroline and 2,2'-Bipyridyl", *Aust. J. Chem.* **1968**, *21*, 631.

[20] J. J. Sletten, A. Soerensen, M. Julve, Y. Journaux, "A Tetranuclear Hydroxo-Bridged Copper(II) Cluster of the Cubane Type. Preparation and Structural and Magnetic Characterization of Tetrakis[(2,2'-Bipyridyl)Hydroxocopper(II)] Hexafluorophosphate", *Inorg. Chem.* **1990**, *29*, 5054–5058.

[21] C. Arcus, K. P. Fivizzani, S. F. Pavkovic, "Preparation of Cu(Tmen)OH(Cl) and Molecular Structure of Di-μ-Hydroxo-Bis(N,N,N′,N′-Tetramethylethylenediamine)-Dicopper(II) Perchlorate, [Cu(Tmen)OH]$_2$(ClO$_4$)$_2$", *J. Inorg. Nucl. Chem.* **1977**, *39*, 285–287.

[22] A. Prescimone, J. Sanchez-Benitez, K. K. Kamenev, S. A. Moggach, J. E. Warren, A. R. Lennie, M. Murrie, S. Parsons, E. K. Brechin, "High Pressure Studies of Hydroxo-Bridged Cu(II) Dimers", *Dalton Trans.* **2009**, *39*, 113–123.

[23] A. Tadsanaprasittipol, H.-B. Kraatz, G. D. Enright, "The Chemistry of Dinitrato-2,2′-Bipyridinecopper(II): Preparation and Characterization of Binuclear Complexes Having a Cu(μ-OH)$_2$Cu and Cu(μ-N$_3$)$_2$Cu Core", *Inorganica Chim. Acta* **1998**, *278*, 143–149.

[24] C. López, R. Costa, F. Illas, C. de Graaf, M. M. Turnbull, C. P. Landee, E. Espinosa, I. Mata, E. Molins, "Magneto-Structural Correlations in Binuclear Copper(II) Compounds Bridged by a Ferrocenecarboxylato(–1) and an Hydroxo- or Methoxo-Ligands", *Dalton Trans.* **2005**, *13*, 2322.

[25] D. Venegas-Yazigi, D. Aravena, E. Spodine, E. Ruiz, S. Alvarez, "Structural and Electronic Effects on the Exchange Interactions in Dinuclear Bis(Phenoxo)-Bridged Copper(II) Complexes", *Coord. Chem. Rev.* **2010**, *254*, 2086–2095.

[26] T. R. Felthouse, E. J. Laskowski, D. N. Hendrickson, "Magnetic Exchange Interactions in Transition Metal Dimers. 10. Structural and Magnetic Characterization of Oxalate-Bridged, Bis(1,1,4,7,7-Pentaethyldiethylene Triamine)Oxalatodicopper Tetraphenylborate and Related Dimers. Effects of Nonbridging Ligands and Counterions on Exchange Interactions", *Inorg. Chem.* **1977**, *16*, 1077–1089.

[27] W. E. Marsh, D. S. Eggleston, W. E. Hatfield, D. J. Hodgson, "Structure and Magnetism in the Chloro-Bridged Copper(II) Complex Di-μ-Chloro-Bis[Chlorobis(4 Methyloxazole)Copper(II)]", *Inorganica Chim. Acta* **1983**, *70*, 137–142.

[28] W. E. Marsh, T. L. Bowman, W. E. Hatfield, D. J. Hodgson, "Synthesis and Structural and Magnetic Characterization of the Dimeric Complex Bis[Dibromobis(4-Methyloxazole)Copper(II)]", *Inorganica Chim. Acta* **1982**, *59*, 19–24.

[29] S. K. Mandal, L. K. Thompson, M. J. Newlands, E. J. Gabe, K. Nag, "Structural and Magnetic Studies on Macrocyclic Dicopper(II) Complexes. Influence of Electron-Withdrawing Axial Ligands on Spin Exchange", *Inorg. Chem.* **1990**, *29*, 1324–1327.

[30] F.-L. Yang, G.-Z. Zhu, B.-B. Liang, Y.-H. Shi, X.-L. Li, "Assembly of Dinuclear Copper(II) Complexes Based on a Tridentate Pyrazol–Pyridine Ligand: Crystal Structures and Magnetic Properties", *Polyhedron* **2017**, *128*, 104–111

[31] D. Venegas-Yazigi, S. Cortés, V. Paredes-García, O. Peña, A. Ibañez, R. Baggio, E. Spodine, "Modulating Magnetic Properties of a Macrocyclic Dinuclear Copper(II) Complex: Influence of Counteranions on the Crystal Structure", *Polyhedron* **2006**, *25*, 2072–2082.

[32] R. P. Doyle, M. Julve, F. Lloret, M. Nieuwenhuyzen, P. E. Kruger, "Hydrogen-Bond Tuning of Ferromagnetic Interactions: Synthesis, Structure and Magnetic Properties of Polynuclear Copper(II) Complexes Incorporating p-Block Oxo-Anions", *Dalton Trans.* **2006**, *17*, 2081–2088.

[33] G. David, N. Ferré, B. Le Guennic, "Consistent Evaluation of Magnetic Exchange Couplings in Multicenter Compounds in KS-DFT: The Recomposition Method", *J. Chem. Theory Comput.* **2023**, *19*, 157–173.

[34] G. Singh, S. Gamboa, M. Orio, D. A. Pantazis, M. Roemelt, "Magnetic Exchange Coupling in Cu Dimers Studied with Modern Multireference Methods and Broken-Symmetry Coupled Cluster Theory", *Theor. Chem. Acc.* **2021**, *140*, 139.

[35] L. Noodleman, "Valence Bond Description of Antiferromagnetic Coupling in Transition Metal Dimers", *J. Chem. Phys.* **1981**, *74*, 5737–5743.

[36] K. Yamaguchi, H. Fukui, T. Fueno, "Molecular Orbital (MO) Theory for Magnetically Interacting Organic Compounds. *Ab-initio* MO Calculations of the Effective Exchange Integrals for Cyclophane-type Carbene Dimers", *Chem. Lett.* **1986**, *15*, 625–628.

[37] G. David, G. Trinquier, J.-P. Malrieu, "Consistent Spin Decontamination of Broken-Symmetry Calculations of Diradicals", *J. Chem. Phys.* **2020**, *153*, 194107.

[38] N. Ferré, N. Guihéry, J.-P. Malrieu, "Spin Decontamination of Broken-Symmetry Density Functional Theory Calculations: Deeper Insight and New Formulations", *Phys. Chem. Chem. Phys.* **2015**, *17*, 14375–14382.

[39] E. Coulaud, N. Guihéry, J.-P. Malrieu, D. Hagebaum-Reignier, D. Siri, N. Ferré, "Analysis of the Physical Contributions to Magnetic Couplings in Broken Symmetry Density Functional Theory Approach", *J. Chem. Phys.* **2012**, *137*, 114106.

[40] E. Coulaud, J.-P. Malrieu, N. Guihéry, N. Ferré, "Additive Decomposition of the Physical Components of the Magnetic Coupling from Broken Symmetry Density Functional Theory Calculations", *J. Chem. Theory Comput.* **2013**, *9*, 3429–3436.

[41] M. Toofan, A. Boushehri, M.-Ul-Haque, "Crystal and molecular structure of di-μ-hydroxo-bis[bipyridylcopper(II)] diperchlorate", *J. Chem. Soc., Dalton Trans*., **1976**, 217-219.

[42] M. Burcak, M. Dusek, K. Fejfarova, M. Spilovsky, I. Potocnak, *CSD Communication*, **2005**.

[43] J.-C. Yao, *CSD Communication*, **2008**.

[44] V. K. Yadav, N. Kumari, L. Mishra, "Reactivity of tricine in the presence of $Cu(ClO4)_2{\cdot}6H_2O$ and 2,2 '-bipyridine: Synthesis, characterization and magnetic property of the complexes", *Indian Journal of Chemistry, Section A: Inorganic,Bio-inorganic, Physical, Theoretical and Analytical Chemistry*, **2011**, *50*, 1035-1042.

[45] B. Saravanan, A. Jayamani, N. Sengottuvelan, G. Chakkaravarthi, V. Manivannan, "Di-μ-hydroxido-κ^4O:O-di-μ-perchlorato-κ^4O:O'-bis[(2,2′-bipyridine-κ^2N,N')copper(II)] ", *Acta Crystallographica Section E: Structure Reports Online*, **2013**, *69*, m600.

[46] A. Jayamani, S. Nagasubramanian, V. Thamilarasan, S. O. Ojwach, G. Gopu, N. Sengottuvelan, "*In-situ* nickel(II) complexes of 3-(dimethylamino)-1-propylamine based Schiff base ligands: Structural, electrochemical, biomolecular interaction and antimicrobial properties", *Inorganica Chim. Acta*, **2018**, *482*, 791-799.

[47] A. Jayamani, N. Sengottuvelan, S. K. Kang, Y.-I. Kim, "Mono- and binuclear copper(II) complexes of the bipyridine ligand: Structural, electrochemical and biological studies", *Polyhedron* **2015**, *98*, 203-216.

[48] R. Guillot, *CSD Communication*, **2018.**

[49] B. Bleaney, K. D. Bowers, "Anomalous Paramagnetism of Copper Acetate", *Proc. R. Soc. Lond. Ser. Math. Phys. Sci.* **1952**, *214*, 451–465.

[50] J. M. Tao, J. P. Perdew, V. N. Staroverov, and G. E. Scuseria, "Climbing the density functional ladder: Nonempirical meta-generalized gradient approximation designed for molecules and solids," *Phys. Rev. Lett.*, **2003**, 91, 146401.

[51] A. D. Becke, "Density-Functional Exchange-Energy Approximation with Correct Asymptotic Behavior", *Phys. Rev. A* **1988**, *38*, 3098–3100.

[52] J. P. Perdew, "Density-Functional Approximation for the Correlation Energy of the Inhomogeneous Electron Gas", *Phys. Rev. B* **1986**, *33*, 8822-8824.

[53] J. P. Perdew, K. Burke, M. Ernzerhof, "Generalized Gradient Approximation Made Simple", *Phys. Rev. Lett.* **1996**, *77*, 3865–3868.

[54] C. Lee, W. Yang, R. G. Parr, "Development of the Colle-Salvetti correlation-energy formula into a functional of the electron density", *Phys. Rev. B: Condens. Matter Mater. Phys.* **1988**, *37*, 785–789.

[55] V. N. Staroverov, G. E. Scuseria, J. Tao, J. P. Perdew, "Comparative Assessment of a New Nonempirical Density Functional: Molecules and Hydrogen-Bonded Complexes", *J. Chem. Phys.* **2003**, *119*, 12129–12137.

[56] (a) E. van Lenthe, E. J. Baerends, J. G. Snijders, "Relativistic Regular Two-component Hamiltonians", *J. Chem. Phys.* **1993**, *99*, 4597–4610. (b) E. van Lenthe, E. J. Baerends, J. G. Snijders, "Relativistic Total Energy Using Regular Approximations", *J. Chem. Phys.* **1994**, *101*, 9783–9792.

[56] A. D. Becke, "Density-Functional Thermochemistry. III. The Role of Exact Exchange", *J. Chem. Phys.* **1993**, *98*, 5648–5652.

[58] J. P. Perdew, Y. Wang, "Accurate and simple analytic representation of the electron-gas correlation energy", *Phys. Rev. B* **1992**, 45, 13244–13249.

[59] S. Grimme, "Accurate Calculation of the Heats of Formation for Large Main Group Compounds with Spin-Component Scaled MP2 Methods", *J. Phys. Chem. A* **2005**, *109*, 3067–3077.

[60] C. Adamo, V. Barone, "Toward Reliable Adiabatic Connection Models Free from Adjustable Parameters", *Chem. Phys. Lett.* **1997**, *274*, 242–250.

[61] C. Adamo, V. Barone, "Toward Reliable Density Functional Methods without Adjustable Parameters: The PBE0 Model", *J. Chem. Phys.* **1999**, *110*, 6158–6170.

[62] M. Ernzerhof, G. E. Scuseria, "Assessment of the Perdew-Burke-Ernzerhof exchange-correlation functional," *J. Chem. Phys.*, **1999**, 110, 5029–5036.

[63] B. A. Heß, C. M. Marian, U. Wahlgren, O. Gropen, "A Mean-Field Spin-Orbit Method Applicable to Correlated Wavefunctions", *Chem. Phys. Lett.* **1996**, *251*, 365–371.

[64] A. D. Becke, "A New Mixing of Hartree–Fock and Local Density-functional Theories", *J. Chem. Phys.* **1993**, *98*, 1372–1377.

[65] S. Grimme, "Semiempirical Hybrid Density Functional with Perturbative Second-Order Correlation", *J. Chem. Phys.* **2006**, *124*, 034108.

[66] H. Iikura, T. Tsuneda, T. Yanai, K. Hirao, "A long-range correction scheme for generalized-gradient-approximation exchange functionals", *J. Chem. Phys.* **2001**, 115, 3540–3544.

[67] J.-D. Chai, M. Head-Gordon, "Long-range corrected hybrid density functionals with damped atom–atom dispersion corrections" *Phys. Chem. Chem. Phys.* **2008**, 10, 6615–6620.

[68] Henry C. Fitzhugh, James W. Furness, Mark R. Pederson, Juan E. Peralta, and Jianwei Sun, "Comparative Density Functional Theory Study of Magnetic Exchange Couplings in Dinuclear Transition-Metal Complexes", *J. Chem. Theory Comput.* **2023,** 19, 5760-5772.

[69] D. A. Pantazis, "Assessment of Double-Hybrid Density Functional Theory for Magnetic Exchange Coupling in Manganese Complexes", *Inorganics* **2019**, *7*, 57.

[70] C. C. J. Roothaan, "Self-Consistent Field Theory for Open Shells of Electronic Systems", *Rev. Mod. Phys.* **1960**, *32*, 179–185.

[71] G. David, F. Wennmohs, F. Neese, N. Ferré, "Chemical Tuning of Magnetic Exchange Couplings Using Broken-Symmetry Density Functional Theory", *Inorg. Chem.* **2018**, *57*, 12769–12776.

[72] I. Castro, J. Faus, M. Julve, M. Verdaguer, A. Monge, E. Gutierrez-Puebla, "Synthesis and Magnetic Properties of Bis(μ-Hydroxo)Bis[(2,2′-Bipyridyl)Copper(II)] Squarate. Crystal Structure of Bis(μ-Hydroxo)Bis[(2,2′-Bipyridyl)Copper(II)] Squarate Tetrahydrate", *Inorganica Chim. Acta* **1990**, *170*, 251–257.

[73] D. Savard, T. Storr, D. B. Leznoff, "Magnetostructural Characterization of Copper(II) Hydroxide Dimers and Coordination Polymers

Coordinated to Apical Isothiocyanate and Cyanide-Based Counteranions", *Can. J. Chem.* **2014**, *92*, 1021–1030.

[74] A. T. Casey, B. F. Hoskins, F. D. Whillan, " The Novel Magnetism and Crystal Structure of the Complex Di- p-hydroxybis(bipyridyl)dicopper(II) Sulphate Pentahydrate", *Chem. Commun.*, **1970**, 904-905.

[75] M. Arakawa-Itoh, K. Tokuman, Y. Mori, T. Kajiwara, M. Yamashita, Y. Fukuda, "Structures and Magnetic Properties of Dinuclear Copper(II) Complexes Containing a Bulky Diamine Ligand, 1,2-Dipiperidinoethane", *Bull. Chem. Soc. Jpn.* **2009**, *82*, 358–363.

[76] G. A. van Albada, I. Mutikainen, U. Turpeinen, J. Reedijk, "Structure, Spectroscopy and Magnetism of a Strong Ferromagnetically Coupled Dinuclear Hydroxo-Bridged Cu(II) Compound with 4,4′-Dimethyl-2,2′-Bipyridine as a Ligand. The First X-Ray Structure of a Dinuclear Cu(II) Compound with Dmbipy", *Inorganica Chim. Acta* **2001**, *324*, 273–277.

[77] S. Youngme, C. Chailuecha, G. A. van Albada, C. Pakawatchai, N. Chaichit, J. Reedijk, "Synthesis, Crystal Structure, Spectroscopic and Magnetic Properties of Doubly and Triply Bridged Dinuclear Copper(II) Compounds Containing Di-2-Pyridylamine as a Ligand", *Inorganica Chim. Acta* **2004**, *357*, 2532–2542.

[78] D. D Lewis, K. T. McGregor, W. E. Hatfield, D. J. Hodgson, "Preparation and Structural and Magnetic Characterization of β-Di-μ-Hydroxo-Bis[2-(2-Dimethylaminoethyl)Pyridine]Dicopper(II) Perchlorate", *Inorg. Chem.* **1974**, *13*, 1013–1019.

[79] P. Chaudhuri, D. Ventur, K. Wieghardt, E.-M. Peters, K. Peters, A. Simon, "Preparation, Magnetism, and Crystal Structures of the Tautomers $[LCu(\mu_2\text{-}OH)_2CuL](ClO_4)_2$ (Blue) and $[LCu(\mu_2\text{-}OH_2)(\mu_2\text{-}O)CuL](ClO\mu_4)\mu_2$ (Green): μ-Aqua-μ-oxo vs. Di-μ-hydroxo Linkage", *Angew. Chem. Int. Ed. Engl.* **1985**, *24*, 57–59.

[80] S. Youngme, G. A. van Albada, O. Roubeau, C. Pakawatchai, N. Chaichit, J. Reedijk, "Synthesis, Crystal Structures and Magnetism of Planar and Roof-Shaped Hydroxo-Bridged Dinuclear Copper(II) Compounds with Di-2-Pyridylamine as a Ligand", *Inorganica Chim. Acta* **2003**, *342*, 48–58.

[81] G. De Munno, M. Julve, F. Lloret, J. Faus, M. Verdaguer, A. Caneschi, "Alternating Ferro- and Antiferromagnetic Interactions in Unusual Copper(II) Chains", *Inorg. Chem.* **1995**, *34*, 157–165.

[82] D. L. Lewis, W. E. Hatfield, D. J. Hodgson, "Crystal and Molecular Structure of α-Di-μ-hydroxo-bis[2-(2-dimethylaminoethyl)pyridine]dicopper(II) Perchlorate", *Inorg. Chem.* **1974**, *13*, 147–152.

[83] K. T. McGreggor, D. J. Hodgson, W. E. Hatfield, "Magnetic Properties of α-Di-μ-hydroxo-bis[2-(2-dimethylaniinoethyl)pyridinecopper(II)] Perchlorate, α-$[Cu(DMAEP)OH]_2(ClO_4)_2$", *Inorg. Chem.* **1976**, *15*, 421–425.

[84] D. A. Clemente, " A study of the 8466 structures reported in Inorganica Chimica Acta: 52 space group changes and their chemical consequences", *Inorganica Chim. Acta* **2005**, *358*, 1725–1748.

[85] J. Mukherjee, R. Mukherjee, "Reaction with dioxygen of a Cu(I) complex of 1-benzyl-[3-(2′-pyridyl)]pyrazole triggers ethyl acetate hydrolysis: acetato-/pyrazolato-, dihydroxo- and diacetato-bridged Cu(II) complexes", *Dalton Trans.*, **2006**, 1611–1621.

[86] E.D. Estes, W. E. Hatfield, D. J. Hodgson, " Structural Characterization of Di-μ-hydroxo-bis(*N, N, N', N'*-tetraethylethylenediamine)dicopper(II) Perchlorate, $[Cu(teen)OH]_2(ClO_4)_2$", *Inorg. Chem.* **1974**, *13*, 1654–1657.

[87] S. Gamboa-Ramírez, "Structure-function relationship in polynuclear bio-inspired copper complexes: Combined experimental and computational studies." Chemical Sciences. Aix Marseille Université, **2023**. https://hal.science/tel-04931252/

[88] O. V. Dolomanov, L. J. Bourhis, R. J. Gildea, J. A. K. Howard, H. Puschmann, "OLEX2: A Complete Structure Solution, Refinement and Analysis Program", *J. Appl. Crystallogr.* **2009**, *42*, 339–341.

[89] G. M. Sheldrick, "SHELXT–Integrated space-group and crystal-structure determination", *Acta Cryst.* **2015**, *A71*, 3–8.

[90] F. Kleemiss, O. V. Dolomanov, M. Bodensteiner, N. Peyerimhoff, L. Midgley, L. J. Bourhis, A. Genoni, L. A. Malaspina, D. Jayatilaka, J. L. Spencer, F. White, B. Grundkötter-Stock, S Steinhauer, D. Lentz, H. Puschmann, S. Grabowsky, "Accurate crystal structures and chemical properties from NoSpherA2", *Chem. Sci.*, **2021**,12, 1675-1692

[91] G. M. Sheldrick, "Crystal structure refinement with SHELXL", *Acta Cryst.* **2015**, *C71*, 3–8.

[92] F. Neese, "Software Update: The ORCA Program System, Version 4.0", *WIREs Comput. Mol. Sci.* **2018**, *8*, e1327.

[93] F. Weigend, R. Ahlrichs, "Balanced Basis Sets of Split Valence, Triple Zeta Valence and Quadruple Zeta Valence Quality for H to Rn: Design and Assessment of Accuracy", *Phys. Chem. Chem. Phys.* **2005**, *7*, 3297–3305.

[94] A. Schäfer, C. Huber, R. Ahlrichs, "Fully Optimized Contracted Gaussian Basis Sets of Triple Zeta Valence Quality for Atoms Li to Kr", *J. Chem. Phys.* **1994**, *100*, 5829–5835.

[95] F. Neese, "An Improvement of the Resolution of the Identity Approximation for the Formation of the Coulomb Matrix", *J. Comput. Chem.* **2003**, *24*, 1740–1747.

[96] F. Weigend, "Accurate Coulomb-Fitting Basis Sets for H to Rn", *Phys. Chem. Chem. Phys.* **2006**, *8*, 1057–1065.

[97] D. A. Pantazis, X.-Y. Chen, C. R. Landis, F. Neese, "All-Electron Scalar Relativistic Basis Sets for Third-Row Transition Metal Atoms", *J. Chem. Theory Comput.* **2008**, 4, 6, 908–919.

[98] Glendening, E. D.; Badenhoop, J. K.; Reed, A. E.; Carpenter, J. E.; Bohmann, J. A.; Morales, C. M.; Landis, C. R.; Weinhold, F. NBO 6.0., **2013**. http://nbo6. chem.wisc.edu/.

[99] M. J. Frisch, G. W. Trucks, H. B. Schlegel, G. E. Scuseria, M. A. Robb, J. R. Cheeseman, G. Scalmani, V. Barone, G. A. Petersson, H. Nakatsuji, X. Li, M. Caricato, A. Marenich, J. Bloino, B. G. Janesko, R. Gomperts, B. Mennucci, H. P. Hratchian, J. V. Ortiz, A. F. Izmaylov, J. L. Sonnenberg, D. Williams-Young, F. Ding, F. Lipparini, F. Egidi, J. Goings, B. Peng, A. Petrone, T. Henderson, D. Ranasinghe, V. G. Zakrzewski, J. Gao, N. Rega, G. Zheng, W. Liang, M. Hada, M. Ehara, K. Toyota, R. Fukuda, J. Hasegawa, M. Ishida, T. Nakajima, Y. Honda, O. Kitao, H. Nakai, T. Vreven, K. Throssell, J. A. Montgomery Jr., J. E. Peralta, F. Ogliaro, M. Bearpark, J. J. Heyd, E. Brothers, K. N. Kudin, V. N. Staroverov, T. Keith, R. Kobayashi, J. Normand, K. Raghavachari, A. Rendell, J. C. Burant, S. S. Iyengar, J. Tomasi, M. Cossi, J. M. Millam, M. Klene, C. Adamo, R. Cammi, J. W. Ochterski, R. L. Martin, K. Morokuma, O. Farkas, J. B. Foresman, D. J. Fox, *Gaussian 09, Revision D.01*, Gaussian, Inc., **2013**.

[100] Chemcraft. http://chemcraftprog.com.

[101] K. T. McGregor, N. T. Watkins, D. L. Lewis, R.F. Drake, D. J. Hodgson, W.E. Hatfield, "Magnetic Properties of Di-μ-Hydroxobis (2,2′-Bipyridyl) Dicopper(II) Nitrate, and the Correlation between the Singlet-Triplet Splitting and the Cu-O-Cu Angle in Hydroxo-Bridged Copper(II) Complexes.", *Inorg. Nucl. Chem. Lett.* **1973**, *9*, 423–428.

[102] O. Kahn, B. Briat, "Exchange Interaction in Polynuclear Complexes. Part 1. Principles, Model and Application to the Binuclear Complexes of Chromium(III)", *J. Chem. Soc. Faraday Trans. 2 Mol. Chem. Phys.* **1976**, *72*, 268–281.

[103] O. Kahn, B. Briat, "Exchange Interaction in Polynuclear Complexes. Part 2. Antiferromagnetic Coupling in Binuclear Oxo-Bridged Iron(III) Complexes.", *J. Chem. Soc. Faraday Trans. 2 Mol. Chem. Phys.* **1976**, *72*, 1441–1446.

[104] P.J. Hay, J. C. Thibeault, R. Hoffmann, "Orbital Interactions in Metal Dimer Complexes." *J. Am. Chem. Soc.* **1975**, *97*, 4884–4899.

Entry for the Table of Contents

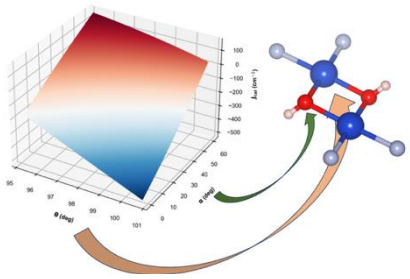

Magneto-structural correlation in bis-μ-hydroxido Cu(II) dimers: the out-of-plane angle (α) of bridging hydroxido groups critically influences the exchange coupling constant (*J*). A three-dimensional correlation combining α and the Cu-OH-Cu angle (θ) enables computationally accurate *J* prediction.